

Cite this: *Phys. Chem. Chem. Phys.*, 2012, **14**, 1860–1864

www.rsc.org/pccp

PAPER

# Faraday rotation and its dispersion in the visible region for saturated organic liquids†

Stefaan Vandendriessche,\* Ventsislav K. Valev and Thierry Verbiest

Received 20th October 2011, Accepted 5th December 2011

DOI: 10.1039/c2cp23311h

Faraday rotation and its dispersion have been measured and calculated in the 400–800 nm wavelength range for a set of saturated organic liquids. The resulting Verdet constants are fitted and trends are analyzed. Comparisons are made to both the polarizability and diamagnetic susceptibility. The data are applied to a connectivity index model, allowing prediction of Verdet constants of aliphatic organic liquids from 400 to 800 nm. The observed correlations and connectivity model improve the understanding of Faraday rotation in diamagnetic materials, allowing for future optimization.

## 1 Introduction

The Faraday effect is a magneto-optical effect in all materials discovered by Michael Faraday.<sup>1</sup> Faraday rotation is the rotation of linearly polarized light in the plane of polarization due to magnetically induced birefringence. It is described by the formula

$$\theta = VBL \quad (1)$$

where  $\theta$  is the polarization rotation,  $V$  is the Verdet constant,  $B$  is the magnetic field parallel to the propagation direction of light and  $L$  is the length of propagation in the dielectricum through the magnetic field. Unlike natural optical rotation, Faraday rotation is non-reciprocal, which means reflections through a sample accumulate rotation and do not cancel out. As such Faraday rotation can be used to design optical switches, modulators, optical isolators<sup>2</sup> and magnetic field sensors.<sup>3</sup>

The Verdet constant  $V$  is a wavelength dependent material property. It is important to make the distinction between the molecular Verdet constant and the Verdet constant of the corresponding liquid. Neglecting solvent effects, both Verdet constants are related by the numerical density  $n$  of the liquid:

$$V_{\text{molecular}} = nV_{\text{liquid}} \quad (2)$$

In regions far from absorption it is possible to write the dependence of the Verdet constant as a quadratic function of the wavelength<sup>4</sup>

$$V = A + \frac{B}{\lambda^2} \quad (3)$$

where  $A$  and  $B$  are fitting parameters and  $\lambda$  is the wavelength.

*Molecular Electronics and Photonics, INPAC, Katholieke Universiteit Leuven, Leuven, Belgium*

† Electronic supplementary information (ESI) available: Measured and calculated Faraday rotation spectra of the organic liquids. See DOI: 10.1039/c2cp23311h

Many calculations of Verdet constants of small organic molecules have been performed with various computational methods,<sup>5–12</sup> and measurements have been performed at various wavelengths for certain organic liquids.<sup>11,13–15</sup> However, to our knowledge no attempt has been made to calculate, measure and model the dispersion of Faraday rotation for a series of organic molecules. As such a total understanding of the Faraday rotation in diamagnetic substances is lacking. We have measured the Faraday rotation and its dispersion for a representative series of branched, unbranched and cyclical alkanes, alcohols and ethers. With the applied connectivity index model it is possible to predict Verdet constants for saturated organic molecules from 400 to 800 nm. This predictive ability and the observed correlations will allow further insight into understanding and optimizing magneto-optical phenomena in diamagnetic materials.

## 2 Experimental

Spectral Faraday rotation measurements were performed using a 150 W Xenon lamp followed by a monochromator. After being linearly polarized, the beam passes through a photo-elastic modulator (Hinds I/FS50) at 45° with respect to the polarization of the light, operating at 50 kHz. Subsequently this beam passes through an optical quartz cuvette with 1 cm path length placed in a DC magnet (HTS-110). Finally the beam passes through a crossed analyzer (90° with respect to the first polarizer). After the beam is detected by a photomultiplier tube, the signal at 100 kHz is analyzed by a lock-in amplifier (SR830). The magnetic field was varied discretely from 0 T to 0.8 T and the signal was measured at each magnetic field. The resulting values were fit linearly to the magnetic field in order to derive the rotation of the sample as a function of the magnetic field.<sup>16</sup> The use of a DC magnetic field avoids the measurement of leakage of the magnetic field

into the photomultiplier tube.<sup>4</sup> Dividing the obtained rotation by the path length of the cell resulted in the Verdet constant of the liquid. The molecular Verdet constant was derived from the Verdet constant of the liquid using the numerical density of the liquid calculated from the molar mass and density from the CRC Handbook of Chemistry and Physics.<sup>17</sup>

Molecular polarizabilities were obtained using the Lorentz–Lorenz equation<sup>5</sup> for refractive indices measured on an Atago DR-A1 Refractometer operating at 589 nm.

Verdet constants were calculated using Dalton<sup>18</sup> with 6-31+G\*\* MP2 FU optimized structures obtained from the CCCBDB.<sup>19</sup> A quadratic response method at the B3LYP/aug-cc-pVDZ approximation was used as described by Botek *et al.*<sup>11</sup>

### 3 Results and discussion

#### 3.1 Trends for alkanes and alcohols

In Fig. 1 and 2 the  $A$  and  $B$  parameters obtained by fitting the calculated and measured molecular Verdet constants to eqn (3) for unbranched alkanes and alcohols are displayed as a function of the number of carbon atoms.

For both  $A$  and  $B$ , a linear trend is observed as a function of the number of carbon atoms, and for both series of compounds the linear fit values are displayed in Table 1. The uncertainty on the  $A$  values is much larger than the uncertainty on the  $B$  values. This is inherent to the dispersion formula (eqn (3)), in which the  $A$  value is a measure of an extrapolation to  $\lambda \rightarrow \infty$ , where the measured values approach 0.

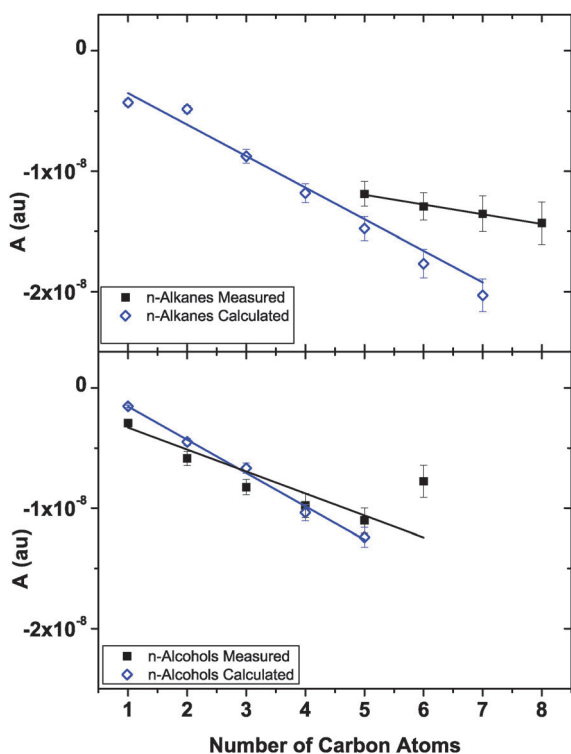


**Fig. 1** The  $A$  parameter from eqn (3) for the calculated and measured Verdet constants of unbranched alkanes and alcohols as a function of the number of carbon atoms. A linear decrease is seen for both the calculated ( $R^2 > 0.97$ ) and the measured ( $R^2 = 0.92$ ,  $R^2 = 0.81$ ) Verdet constants as a function of the number of carbon atoms.

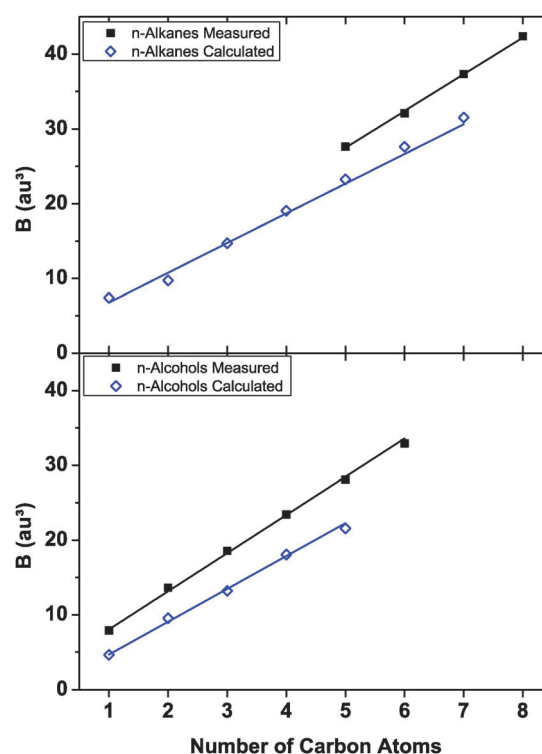


**Fig. 2** The  $B$  parameter from eqn (3) for the calculated and measured Verdet constants of unbranched alkanes and alcohols as a function of the number of carbon atoms. A linear increase ( $R^2 > 0.97$ ) is seen for both the calculated and the measured Verdet constants as a function of the number of carbon atoms.

**Table 1** Results of the linear fit of the  $A$  and  $B$  parameters for calculated and measured unbranched alkanes and alcohols as a function of the number of carbon atoms

	Unbranched alkanes	Unbranched alcohols
Slope of measured $A$ values	$-0.81 \times 10^{-9}$ au	$-1.83 \times 10^{-9}$ au
Slope of calculated $A$ values	$-2.62 \times 10^{-9}$ au	$-2.77 \times 10^{-9}$ au
Slope of measured $B$ values	$4.91$ au <sup>3</sup>	$5.11$ au <sup>3</sup>
Slope of calculated $B$ values	$3.98$ au <sup>3</sup>	$4.40$ au <sup>3</sup>

All the slopes of calculated values are smaller than the slopes of measured values. This corresponds well to the known tendency of quadratic response calculations performed at the B3LYP/aug-cc-pVDZ level to result in lower calculated Verdet constants than measured.<sup>11</sup> For the unbranched alkanes, a 20% smaller slope is obtained for the calculated  $B$  values than for the measured  $B$  values. This underestimation is reduced to 15% for the unbranched alcohols. The slope of the measured  $B$  values is very similar for both series. Combined with the observed linear trend as a function of the number of carbon atoms this leads to the postulation of an additive model, where each additional  $\text{CH}_2$  moiety contributes equally to the Verdet constant. While this is applicable to linear chain length extension, it is necessary to take into account longer-range interactions and changes in molecular structure in order to predict the Verdet constants of arbitrary molecules. This is further investigated in Section 3.4. There is a deviation from the linear trend expected for the additive model in the experimental  $A$  values of

the unbranched alcohols, which is attributed to intermolecular interactions such as hydrogen bonding. This explanation is supported by the observation that the linear trend is present in the calculated  $A$  values for the unbranched alcohols, which neglect intermolecular interactions. Additionally no deviation is observed for the experimental  $A$  values of the unbranched alkanes, for which intermolecular interactions are expected to be smaller than in the unbranched alcohols.

### 3.2 Relation to the diamagnetic susceptibility

It is interesting to compare Faraday rotation to diamagnetic susceptibility.<sup>17</sup> While this comparison has already been made for parameters of the macroscopic Verdet constant of the liquid,<sup>15</sup> it is more instructive to compare the diamagnetic susceptibility to fits to the microscopic, molecular Verdet constant. The Verdet constants of a variety of saturated organic liquids, including alkanes, alcohols and ethers, were calculated and measured over the 400–800 nm wavelength region.† The resulting  $A$  and  $B$  parameters are shown in Fig. 3.

A linear correlation between both parameters and the diamagnetic susceptibility is observed. However, the correlation is significantly stronger for the  $B$  parameter (calculated value:  $R^2 = 0.889$ , measured value:  $R^2 = 0.978$ ) than for the  $A$  parameter (calculated value:  $R^2 = 0.793$ , measured value:  $R^2 = 0.811$ ). The weaker fit for the  $A$  parameter is due to the inherent lower precision of the  $A$  parameter, as described in Section 3.1. Again we observe a smaller slope for the calculated  $B$  values ( $0.444 \times 10^6 \text{ mol au}^3 \text{ cm}^{-3}$ ) than for the

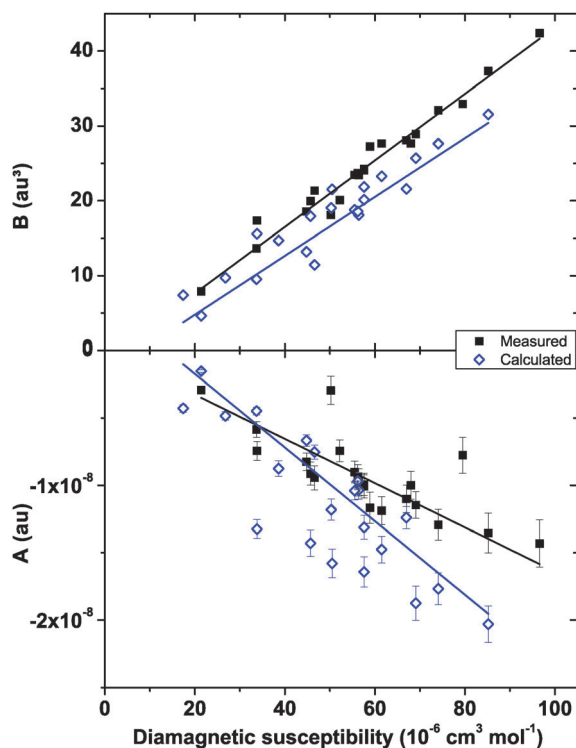


**Fig. 3** The  $A$  and  $B$  parameters from eqn (3) for the calculated and measured Verdet constants of a variety of aliphatic liquids as a function of the diamagnetic susceptibility. A linear relation is seen for both the calculated and the measured Verdet constants, with a stronger correlation seen for the  $B$  parameter.

measured  $B$  values ( $0.393 \times 10^6 \text{ mol au}^3 \text{ cm}^{-3}$ ). The weaker correlation for the calculated values can be understood in terms of the chosen basis set for the calculations. When basis sets with a larger number of valence orbitals are chosen, the value of the calculated Verdet constant approaches the measured one at a different rate for calculations with different numbers of electrons and orbitals. As such at a given level of approximation, the deviation from the infinite orbital limit value of the Verdet constant for this type of calculation differs per molecule, and this weakens the observed correlation. The chosen level of approximation provides sufficient accuracy to reproduce the trends. Higher levels of approximation provide higher accuracy, but due to the slow convergence of magneto-optical calculations with the increase of number of orbitals,<sup>10</sup> the computational time-accuracy trade off favors the employed approximation.

### 3.3 Relation to the molecular polarizability

The Bequerel formula predicts a linear relation between the derivative of the polarizability to the frequency<sup>8</sup> and the Verdet constant at that frequency. Data on the dispersion of refractive indices are however difficult to obtain accurately. The refractive index on the other hand is relatively simple to determine. Despite the fact that the refractive index and molecular polarizability are not used in the calculation of the Faraday rotation from the measured data, we also observe a linear relation between the molecular polarizability and the molecular Verdet constant at the same wavelength, displayed in Fig. 4.

A larger slope ( $291 \times 10^{-11} \text{ au}^3$  with  $R^2 = 0.985$ ) is obtained for the measured  $B$  values than for the calculated  $B$  values ( $253 \times 10^{-11} \text{ au}^3$  with  $R^2 = 0.911$ ). This correlation provides a practical method for estimating Verdet constants at a specific wavelength, given the ease of measuring the refractive index using a refractometer.

More interestingly, a correlation was also found between the molecular polarizability at 589 nm and the  $A$  and  $B$  parameters of eqn (3) (Fig. 5). Once more the linear trend is stronger for the  $B$  values than for the  $A$  values, for the same reasons explained in Section 3.1.

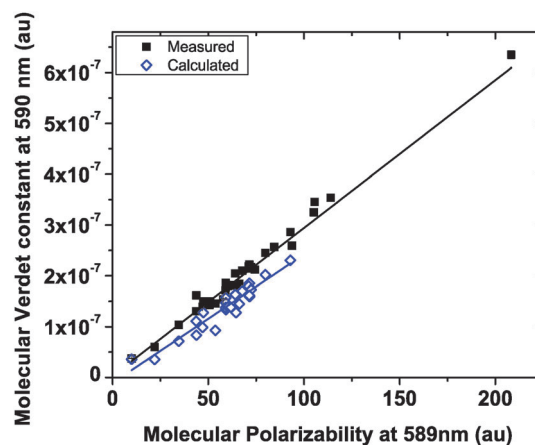


**Fig. 4** The Verdet constant at 590 nm as a function of the molecular polarizability at 589 nm. A linear relation is seen for both the calculated and the measured Verdet constants.

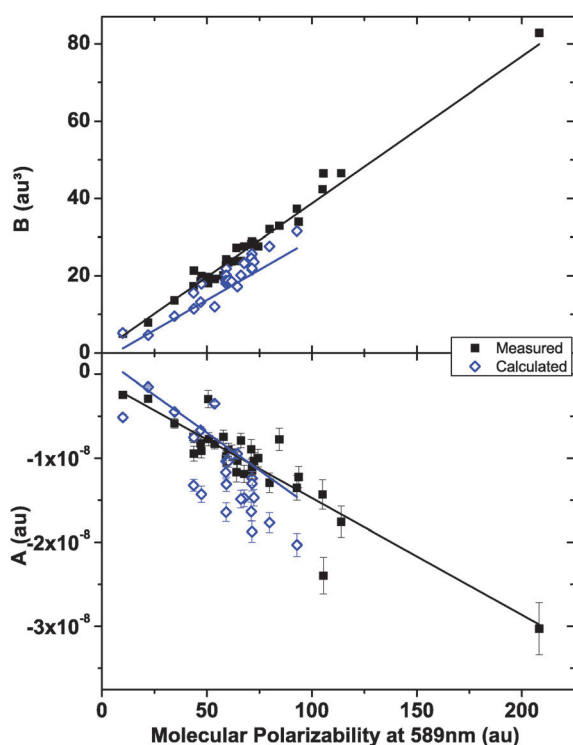


**Fig. 5** The  $A$  and  $B$  parameters from eqn (3) for the calculated and measured Verdet constants as a function of the molecular polarizability at 589 nm. A linear relation is seen for both the calculated and the measured Verdet constants.

This relationship allows the prediction of the Verdet constant of a liquid over a wide wavelength range with a single measurement of a refractive index at an arbitrary wavelength.

### 3.4 Modeling the Verdet constant

While the linear relation to the diamagnetic susceptibility and molecular polarizability allows for accurate estimates of the Verdet constant, these variables are not sufficient to fully explain the observed Verdet constant. This is illustrated by

1-butanol and 2-butanol, both of which have a molecular polarizability of  $59.14 \pm 0.34$  au, but respective  $B$  parameters of  $23.44 \pm 0.14$  au<sup>3</sup> and  $24.26 \pm 0.11$  au<sup>3</sup>.

Due to the observed correlation between the diamagnetic susceptibility and the  $B$  parameter of the Verdet constant fit, it is most obvious to investigate a modified model for the prediction of the diamagnetic susceptibility. The most straightforward model is to decompose the molecule into fragments and, using Pascal's constants,<sup>20</sup> assign each a contribution to the diamagnetic susceptibility of the molecule. Because this model decomposes 1-butanol and 2-butanol into the same fragments, it also fails to distinguish between these two molecules; as such it is necessary to apply a more complex model.

To account for effects over more than one bond, a molecular connectivity index model is applied. A recent connectivity index, designed for the modeling of diamagnetic susceptibilities,<sup>21</sup> has been chosen. The details on molecular connectivity indices are beyond the scope of this paper and can be found elsewhere.<sup>22</sup> The  $n$ -th order molecular connectivity index  ${}^n\chi_k$  can be written as

$${}^n\chi_k = \sum_{j=1}^{N_n} \left( \prod_{i=1}^{n+1} \frac{1}{\sqrt{\delta'_i}} \right) \quad (4)$$

where  $n$  is the order of the molecular connectivity index,  $k$  is a contiguous path type of fragment,  $N_n$  is the number of relevant paths and  $\delta'_i$  is the chosen atomic connectivity index. To illustrate the calculation of the molecular connectivity indices we take ethanol as an example. The zeroth order molecular connectivity index can be calculated as follows

$${}^0\chi_k = \frac{1}{\sqrt{\delta'_C}} + \frac{1}{\sqrt{\delta'_C}} + \frac{1}{\sqrt{\delta'_O}} \quad (5)$$

essentially adding up the contribution of each non-hydrogen atom. The first order molecular connectivity index is

$${}^1\chi_k = \frac{1}{\sqrt{\delta'_C\delta'_C}} + \frac{1}{\sqrt{\delta'_C\delta'_O}} \quad (6)$$

**Table 2** The  $B$  parameter from fits to measured Faraday rotation compared to the predicted  $B$  value. A good agreement is seen between the predicted and measured values

	$B$ from measurements/au <sup>3</sup>	Predicted $B$ /au <sup>3</sup>		$B$ from measurements/au <sup>3</sup>	Predicted $B$ /au <sup>3</sup>
Methanol	7.893	7.979	THF	19.180	20.930
Ethane		11.864	1,4-Dioxane	20.100	22.954
Ethanol	13.643	12.828	Pentane	27.646	26.196
Dimethylether		13.825	Cyclopentane	23.723	23.656
Propane		16.742	1-Pentanol	28.094	27.124
Propanol	18.569	17.623	2-Pentanol	28.909	27.995
Isopropanol	19.951	18.554	3-Pentanol	28.252	27.932
Methoxyethane		18.584	THP	23.874	25.680
Propylene glycol	19.756	19.442	MTBE	28.385	30.329
1,3-Propanediol	18.102	18.551	3-methyl-1-butanol	28.971	28.084
Acetone	17.360	17.002	Hexane	32.103	30.946
Butane		21.446	Hexanol	32.926	31.874
Isobutane		22.539	Cyclohexane	27.647	28.407
1-Butanol	23.436	22.373	2-methoxyethylether	33.986	36.848
2-Butanol	24.257	23.224	Heptane	37.328	35.697
Isobutanol	24.059	23.353	Octane	42.399	40.447
Methoxypropane	22.691	23.385	Isooctane	46.501	43.731
Diethylether	23.469	23.369	Diocylether	82.823	80.474
1,2-Dimethoxyethane	23.911	25.324			

quantifying the contribution of each bond. The second order molecular connectivity index is

$${}^2\chi_k = \frac{1}{\sqrt{\delta'_C \delta'_C \delta'_O}} \quad (7)$$

which is the contribution of the two-bond fragment C–C–O.

We have chosen an atomic connectivity index  $\delta'_i$  designed by Mu *et al.*<sup>21</sup> which takes into account the chemical environment of the atom

$$\delta'_i = \left( \frac{Z_i^v - h_i}{Z_i - Z_i^v - 1} \right) \left( \frac{x_i}{x_{C-sp^3}} \right) \quad (8)$$

where  $Z_i^v$  and  $Z_i$  are respectively the number of valence and total electrons on atom  $i$ ,  $h_i$  is the number of hydrogen atoms connected to atom  $i$ ,  $x_i$  is the orbital electronegativity of atom  $i$  and  $x_{C-sp^3}$  is the orbital electronegativity of an  $sp^3$  hybridized carbon atom. The orbital electronegativity is defined as

$$x_i = -\frac{\alpha \varepsilon_s + (1 - \alpha) \varepsilon_p}{4.95} \quad (9)$$

where  $\alpha$  is the composition of the s orbital and  $\varepsilon_s$  and  $\varepsilon_p$  are the energies of, respectively, the s and p orbitals.

Fitting of the chosen connectivity index to the  $B$  parameters obtained by fitting of the experimental Faraday rotation data yields

$$B = -0.09531 + 5.13093^0\chi_k + 1.69778^1\chi_k + 0.77308^2\chi_k \quad (10)$$

with  $R^2 = 0.987$ . The measured and predicted  $B$  values are displayed in Table 2.

A good agreement is seen between the  $B$  values from measurements and the predicted values. For the  $A$  parameter a much weaker fit is seen, and due to the small influence on the Verdet constant (typically less than 5% at the measured wavelengths) it is not included in the model. The  ${}^2\chi_k : {}^1\chi_k$  ratio is 0.46, indicating a significant contribution of two-bond fragments. Despite this the single atom contributions, quantified by  ${}^0\chi_k$ , remain dominant, in agreement with the observed additivity in Section 3.1. However, the largest deviation in our model is observed for the ring systems, suggesting that higher order fragments play a non-negligible role in Faraday rotation of diamagnetic substances. As such, future investigations with larger data sets will need to include higher order molecular connectivity indices.

## 4 Conclusions

We have measured the Faraday rotation of various saturated organic liquids between 400 nm and 800 nm, and the resulting values correspond well to previously reported values. From these measurements we have calculated the molecular Verdet constant. By fitting these data to a dispersion formula for Verdet constants sufficiently far from resonance, we are able to quantify the Verdet constant over a broad wavelength region. The Verdet constant shows trends over the alkane and alcohol carbon backbone length. Additionally, a linear correlation

to both the molecular polarizability and the diamagnetic susceptibility is observed. For further refinement, we apply a molecular connectivity index model based on our measurements in order to predict the Verdet constant of arbitrary aliphatic compounds. With knowledge of the density of the liquid, this allows the prediction of the Faraday rotation of arbitrary aliphatic liquids at a chosen wavelength. The results reveal important contributions of large fragments in the molecules to the Faraday rotation. The ability to predict the Verdet constants and the observed correlations further allow for optimization and a better understanding of magneto-optical phenomena in diamagnetic materials.

## Acknowledgements

S.V. and V.K.V. are grateful for the financial support from the FWO-Vlaanderen. We are grateful to the University of Leuven (GOA) for financial support. We would like to thank M. K. Vanbel, W. Brulot and M. Bloemen for the useful discussions, input and careful proofreading.

## References

- 1 M. Faraday, *Experimental Researches in Electricity*, R. Taylor & W. Francis, 1839–1855, vol. III.
- 2 G. W. Day, D. N. Payne, A. J. Barlow and J. J. Ramskov-Hansen, *Opt. Lett.*, 1982, **7**, 238–240.
- 3 D. Budker, D. F. Kimball, S. M. Rochester, V. V. Yashchuk and M. Zolotarev, *Phys. Rev. A*, 2000, **62**, 043403.
- 4 A. Jain, J. Kumar, F. Zhou and L. Li, *Am. J. Phys.*, 1999, **67**(8), 714–717.
- 5 P. Jørgensen, J. Oddershede and N. H. F. Beebe, *J. Chem. Phys.*, 1978, **68**, 2527–2532.
- 6 D. M. Bishop and S. M. Cybulski, *J. Chem. Phys.*, 1990, **93**, 590–599.
- 7 W. A. Parkinson, S. P. A. Sauer, J. Oddershede and D. M. Bishop, *J. Chem. Phys.*, 1993, **98**, 487–495.
- 8 S. Coriani, C. Hättiga, P. Jørgensen, A. Halkier and A. Rizzo, *Chem. Phys. Lett.*, 1997, **281**, 445–451.
- 9 S. Coriani, P. Jørgensen, O. Christiansen and J. Gauss, *Chem. Phys. Lett.*, 2000, **330**, 463–470.
- 10 M. Krykunov, A. Banerjee, T. Ziegler and J. Autschbach, *J. Chem. Phys.*, 2005, **122**, 074105.
- 11 E. Botek, B. Champagne, T. Verbiest, P. Gangopadhyay and A. Persoons, *ChemPhysChem*, 2006, **7**, 1654–1656.
- 12 E. Botek, B. Champagne, P. Gangopadhyay, A. Persoons and T. Verbiest, *Comput. Lett.*, 2007, **3**, 193–200.
- 13 A. B. Villaverde and D. A. Donatti, *J. Chem. Phys.*, 1979, **71**, 4021–4024.
- 14 K. Isai, M. Suwa and H. Watarai, *Anal. Sci.*, 2009, **25**, 1–3.
- 15 S. Egami and H. Watarai, *Rev. Sci. Instrum.*, 2009, **80**, 093705.
- 16 V. K. Valev, J. Wouters and T. Verbiest, *Am. J. Phys.*, 2008, **76**, 626–629.
- 17 *CRC Handbook of Chemistry and Physics, 90th Edition*, ed. D. R. Lide, CRC Press, 2009.
- 18 DALTON, a molecular electronic structure program, Release Dalton2011 (2011), see <http://daltonprogram.org/>.
- 19 NIST Computational Chemistry Comparison and Benchmark Database, NIST Standard Reference Database Number 101 Release 15b, August 2011, Editor: Russell D. Johnson III <http://cccbdb.nist.gov/>.
- 20 G. A. Bain and J. F. Berry, *J. Chem. Educ.*, 2008, **85**, 532.
- 21 L. Mu, C. Feng and H. He, *Ind. Eng. Chem. Res.*, 2008, **47**, 2428–2433.
- 22 L. Kier and L. Hall, *Molecular connectivity in chemistry and drug research*, Academic Press, 1976.